Multidiciplinary Output Research For Actual and International Issue (MORFAI Journal) ISSN (e): 2808-6635
Volumes 6 No. 4 (2026)

COMPUTATIONAL EVALUATION OF CRITICAL WEAR LIMITS IN FORKLIFT FORK ARMS USING THE FINITE ELEMENT METHOD: TOYOTA 5FD70 CASE STUDY

Aminuddin[1]*, Rasyid Ridho Haharaha[2], Oloan[3], Arif Rahman Hakim
University of Riau Kepulauan, Batam, Indonesia
E-mail: amintribun@gmail.com [1]*, rasyidridhoharahap@gmail.com[2], oloanritonga707@gmail.com[3], arhakim88yahoo.com[4]

Received : 01 April 2026 Accepted : 05 May 2026
Revised : 10 April 2026 Published : 16 June 2026

Abstract

Forklift fork arms are critical load-bearing components that experience progressive thickness reduction due to operational abrasion. Indonesian Ministry of Manpower Regulation No. 08/2020 and ISO 5057:2022 require fork withdrawal when blade thickness is reduced to 90% of its original value. However, conventional inspection does not explain the continuous evolution of structural safety margins. This study evaluates the safety margin degradation of Toyota 5FD70 forklift fork arms under three wear scenarios using linear static Finite Element Method (FEM). The model geometry was developed from dimensional data in a certified inspection report. The material was modeled as AISI 4140 quenched and tempered steel with a conservative yield strength of 850 MPa. Numerical validity was checked through a mesh convergence study, reaching a final deviation of 1.98%. The results show that all static scenarios remain in the elastic regime, with Safety Factors of 1.745 at 0% wear, 1.759 at 5% wear, and 1.607 at 10% wear. A dynamic projection at 10% wear with a Dynamic Amplification Factor of 1.30 reduced the Safety Factor to 1.235, which falls into the marginal zone. These findings support the 10% wear limit as an early-warning threshold for risk-based forklift fork integrity management.

Keywords: Finite Element Method; Forklift Fork Arms; Safety Factor; Von Mises Stress.

INTRODUCTION

Finite Element Analysis (FEA) enables quantitative evaluation of stress distribution in mechanical components and is widely used to assess structural integrity. In forklift systems, the fork arm is one of the most critical components because it works as a cantilever beam. The shank acts as the support, while the blade carries the lifted load at a specified load center. This configuration concentrates the largest bending moment in the heel region, especially around the inner heel radius. During daily operation, the lower surface of the blade also experiences repeated contact with floors and pallets. This contact accelerates abrasion and reduces the effective blade thickness. Previous failure analysis studies have reported forklift fork failures caused by wear, repeated loading, overload, and fatigue-related mechanisms (Figueiredo et al., 2001; Massone & Boeri, 2010; Pantazopoulos et al., 2014). From a mechanics perspective, blade thinning does not merely reduce the physical dimension. According to Euler-Bernoulli beam theory, maximum bending stress is inversely proportional to the square of the section thickness. Therefore, a 10% reduction in thickness can increase bending stress by approximately 23.5%. This relationship explains why a relatively small wear depth in a load-bearing component can produce a significant reduction in the safety margin.

Indonesian Ministry of Manpower Regulation No. 08/2020 and ISO 5057:2022 Clause 5.7.1 require fork arms to be withdrawn from service when blade thickness is reduced to 90% of the original thickness, especially in the heel region. In practice, fitness for service is verified through physical dimensional measurement, a 110% Safe Working Load (SWL) static load test under ISO 2330:2002, and Magnetic Particle Inspection (MPI). These procedures are important and practical. However, they do not visualize how the Safety Factor changes continuously under different wear scenarios. This information gap matters for companies that apply risk-based asset management. This study aims to evaluate the structural safety margin degradation of a Toyota 5FD70 forklift fork arm with a rated capacity of 7,000 kg using linear static FEM. The study makes two main contributions. First, it provides a mechanics-based verification of the 10% wear limit stated in Permenaker No. 08/2020 and ISO 5057:2022. Second, it combines certified field inspection data, mesh convergence validation, and a Dynamic Amplification Factor (DAF) projection to assess Safety Factor evolution from nominal condition to the critical wear threshold. $\sigma max = M c / I = 6 F L / (b h^2)$

LITERATURE REVIEW

Forklift fork arms are critical structural components in material handling systems because they directly carry the lifted load and transfer bending forces to the forklift carriage. The mechanical behavior of a fork arm is commonly interpreted as a cantilever structure, where the shank acts as the restrained support and the blade receives the external load at a specified load center. This configuration produces maximum bending stress near the heel region, especially around the inner heel radius where geometry changes sharply. Classical stress analysis shows that bending stress increases when the effective section modulus decreases, making blade thickness an important variable in fork integrity evaluation (Young, Budynas, & Sadegh, 2011). Stress concentration theory also confirms that local geometric discontinuities, such as curved heel regions and section transitions, may increase local stress beyond the nominal analytical value (Pilkey & Pilkey, 2008).

Previous failure analysis studies provide important evidence that forklift fork failure is rarely caused by a single factor. Figueiredo et al. (2001) investigated the fracture of heavy-duty lift truck forks and found that local defects, welded regions, and dynamic effects may contribute to premature failure. Massone and Boeri (2010) reported that abusive service conditions, overloading, and inappropriate operational practices may initiate fatigue cracks in forklift forks. Pantazopoulos et al. (2014) further showed that abnormal fatigue failure in forklift forks can be followed by sudden overload fracture. These studies are useful because they clarify the failure mechanisms after damage has occurred. However, they provide limited explanation of how the safety margin changes progressively before visible failure or crack indication appears.

Wear is one of the most important degradation mechanisms in fork arms because it reduces the effective blade or shank thickness. ISO 5057:2022 requires fork arms to be withdrawn from service when the blade or shank thickness is reduced to 90% of its original thickness, with special attention to the heel region (ISO, 2022). This requirement is consistent with practical fork safety guidance that treats 10% thickness loss as a replacement threshold because it significantly reduces fork capacity (Cascade Corporation, 2018). ISO 2330:2002 also establishes manufacturing, testing, and marking requirements for solid-section fork arms, including yield, impact, and fatigue testing provisions (ISO, 2002). These standards provide a clear inspection basis. However, they do not fully explain the continuous mechanical relationship between wear progression, stress increase, and Safety Factor reduction.

Finite Element Method offers a useful approach to overcome this limitation because it can represent complex geometry, local stress concentration, and three-dimensional stress distribution. FEM is widely used in engineering analysis because it allows structural components to be discretized into smaller elements and solved numerically under specified boundary and loading conditions (Bathe, 2014). The accuracy of FEM results depends strongly on element type, boundary conditions, and mesh refinement, especially in areas with high stress gradients (Zienkiewicz, Taylor, & Zhu, 2013). In fork arm analysis, the heel region requires refined meshing because it is the main stress concentration zone. Therefore, a mesh convergence study is necessary to ensure that the maximum Von Mises stress is not merely a numerical artifact.

The Von Mises criterion is appropriate for evaluating ductile steel components because it estimates yielding under multiaxial stress states. Fork arms are commonly made from forged steel or alloy steel, which generally behaves as a ductile material under static loading. Safety Factor can be calculated by comparing the material yield strength with the maximum Von Mises stress obtained from FEM (Dowling, 2013). AISI 4140 quenched and tempered steel is often used as a representative high-strength alloy steel for heavy-duty mechanical components because it provides high yield strength, toughness, and fatigue resistance (ASM International, 1990). Nevertheless, when the exact fork material grade is not available from the inspection document, material selection must be treated conservatively. A sensitivity analysis is required to evaluate whether the safety conclusion remains valid under possible yield strength variation.

Dynamic loading is also relevant because forklift operation does not always occur under purely static conditions. Forklifts may experience inertial effects during lifting, travelling, braking, and load handling on uneven surfaces. EN 13001-2:2021 explains that dynamic factors are used in lifting equipment design to account for load effects caused by hoisting, acceleration, travelling, and other operational actions (CEN, 2021). Although this standard is developed for crane design rather than forklift-specific fork evaluation, the concept of dynamic amplification remains useful as a conservative projection. This approach should not be interpreted as a substitute for full transient dynamic simulation. It is better understood as a preliminary risk-based estimate of how dynamic effects may reduce the static Safety Factor.

Recent computational tools also support the practical application of FEM in industrial component evaluation. PrePoMax is an open-source pre- and post-processor for the CalculiX FEM solver and supports the preparation of Abaqus-compatible input decks (Borovinšek, 2025). CalculiX is a three-dimensional finite element solver that supports linear, nonlinear, static, dynamic, and thermal analyses using an Abaqus-like input format (Dhondt, 2024). These tools make FEM-based structural assessment more accessible for engineering inspection and asset integrity evaluation. Their use is particularly relevant for components such as forklift fork arms, where inspection data can be transformed into a computational model to estimate stress distribution and remaining safety margin.

Based on the reviewed literature, three research gaps can be identified. First, existing forklift fork studies mainly emphasize post-failure diagnosis, while fewer studies evaluate progressive safety margin degradation under controlled wear scenarios. Second, inspection standards clearly define the 10% wear limit, but they do not provide a continuous stress-based explanation of how the Safety Factor changes from nominal thickness to the withdrawal threshold. Third, limited studies integrate certified field inspection data, mesh-converged FEM, conservative material modelling, material sensitivity analysis, and dynamic amplification projection in one assessment framework. This study addresses these gaps by evaluating Toyota 5FD70 fork arms under 0%, 5%, and 10% wear scenarios. The study positions FEM as a decision-support method that complements field inspection and provides a mechanics-based explanation of the regulatory 10% wear limit.

METHOD

2.1. Study Object and Unit Specifications

The study object was a pair of lifting fork arms installed on a Toyota 5FD70 diesel forklift owned by a company in the oil and gas fabrication and infrastructure service sector. The unit underwent periodic inspection under Indonesian Ministry of Manpower Regulation No. 08/2020. The technical and dimensional specifications are summarized in Table 1.

Table 1. Technical specifications of the unit and fork arms based on the inspection report

Parameter	Actual Data
Make / Type	Toyota 5FD70
Serial number	A5FD70-31016
Capacity (SWL)	7,000 kg @ LC 600 mm
Drive type	Diesel (14Z-II Engine)
Blade dimensions (L x W x T)	1,200 x 120 x 60 mm
Material type	Forged carbon steel
Load center (LC)	600 mm
110% SWL load test	Satisfactory, no permanent deformation
NDT MPI	No indication - pass

2.2. Software

The computational workflow used three software tools: (i) SolidWorks 2023 SP5 for three-dimensional geometry modeling, (ii) PrePoMax v2.4.0 (Borovinsek, 2025) as the pre-processing and post-processing interface for the CalculiX solver, and (iii) CalculiX v2.22 as the FEM solver with Abaqus-compatible .inp input format.

2.3. Material Properties

The inspection record identified the fork material as forged carbon steel without a specific metallurgical grade. AISI 4140 quenched and tempered (Q&T) steel was selected for the simulation because its mechanical and metallurgical characteristics are consistent with heavy-duty forged steel applications and are well documented in previous studies (Badaruddin et al., 2023; Simunovic et al., 2024). The selected yield strength was $\sigma y = 850$ MPa, used as a conservative calibrated value because the field load test at 110% SWL showed no permanent deformation (PT Dalaz Asset Integrity Management, 2025a). The material properties used in the FEM model are listed in Table 2.

Table 2. AISI 4140 Q&T material properties used as FEM inputs

Property	Value	Unit	Reference
E, modulus of elasticity	205	GPa	ASM International (1990)
ν, Poisson ratio	0.28	-	ASM International (1990)
σy, conservative value	850	MPa	ASM International (1990)
σy, AISI 4140 Q&T range	655-900	MPa	ASM International (1990)
σu, ultimate tensile strength	1,020	MPa	ASM International (1990)
ρ, density	7,850	kg/m3	ASM International (1990)

2.4. Geometry Modeling, Meshing, and Convergence

The fork geometry was modeled according to the actual measured dimensions from the certified inspection report. The analysis used C3D10 elements, namely second-order ten-node quadratic tetrahedral solid elements. These elements were selected because their quadratic shape functions can capture high stress gradients around the inner heel radius more accurately than first-order tetrahedral elements (Bathe, 2014; Zienkiewicz et al., 2013). A multi-zone mesh strategy was applied. A local element size of 1.5 mm was used in the critical inner heel radius, while a larger element size of 6.0-8.0 mm was used along the blade body. Mesh independence was checked through four refinement iterations, as summarized in Table 3 and Figure 1. The final model used 163,986 elements and reached a convergence deviation of 1.98%, which met the selected threshold of less than 2%.

Table 3. Mesh convergence study for the baseline 0% wear scenario

Iteration	Number of elements	σVM,max (MPa)	Deviation (%)	Status
1, coarse	42,000	544	-	-
2	95,000	463	14.89	-
3	140,000	478	3.24	-
4, final	163,986	487.1	1.98	Converged

2.5. Boundary Conditions and Loading

The rear surface of the shank was assigned a fixed support boundary condition. For a three-dimensional solid element model, this condition constrains translational degrees of freedom in the x, y, and z directions. Rotational degrees of freedom are not directly assigned to C3D10 solid elements because the nodes only have translational degrees of freedom. This boundary condition represents a conservative upper-bound stiffness idealization of the support. It provides a lower-bound estimate of the Safety Factor.

The applied force was calculated per fork arm because the total forklift capacity is shared by two fork arms under symmetric loading. The 100% SWL force per fork was 34,335 N, and the 110% SWL load test force per fork was 37,770 N.

$F100 = (7{,}000 \text{ kg} \times 9.81 \text{ m/s}^2) / 2 = 34{,}335$ N per fork

$F110 = 1.10 \times F100 = 37{,}770$ N per fork

A Dynamic Amplification Factor (DAF) of 1.30 was adopted as a conservative estimate based on the analogy of $\varphi 2 = 1 + \beta 2\ vh$ from EN 13001-2:2021. With the actual lifting speed vh = 0.48 m/s and the assumed stiffness class HC4 (β2 = 0.68), φ2 is approximately 1.33. This value was rounded to 1.30 for conservative projection. The forklift-specific standards used in this study do not provide an explicit DAF formulation for structural analysis. Therefore, $\sigma eff = \sigma FEM \times DAF$ was treated as a conservative projection, not as a result of full transient dynamic simulation.

2.6. Wear Scenarios

Three blade thickness scenarios were simulated to represent nominal, intermediate, and critical wear conditions. The baseline thickness was 60.0 mm. A 5% wear condition reduced the thickness to 57.0 mm. A 10% wear condition reduced the thickness to 54.0 mm, corresponding to the maximum permissible wear threshold under Permenaker No. 08/2020 and ISO 5057:2022 Clause 5.7.1. The scenarios are listed in Table 4.

Table 4. Fork blade thickness variation scenarios

Scenario	Wear level	h (mm)	Criterion basis
Baseline, Sc.1	0%	60.0	Measured nominal dimension (PT Dalaz, 2025a)
Intermediate, Sc.2	5%	57.0	Midpoint toward the critical limit
Critical, Sc.3	10%	54.0	Maximum limit under Permenaker No. 08/2020 and ISO 5057:2022 Clause 5.7.1

2.7. Structural Evaluation Criteria

Structural evaluation used the Von Mises yield criterion, which is appropriate for ductile steels such as AISI 4140 Q&T (Dowling, 2013). The Safety Factor was calculated as the ratio between the conservative yield strength and the maximum Von Mises stress. The interpretation scale for the static Safety Factor is presented in Table 5.

$$\sigma_{VM} = \sqrt{[(\sigma_1 - \sigma_2)^2 + (\sigma_2 - \sigma_3)^2 + (\sigma_3 - \sigma_1)^2] / 2}$$

$$SF = \sigma_y / \sigma_{VM,max}$$

Table 5. Static Safety Factor interpretation scale

SF value	Classification	Operational implication
>= 2.00	Very safe	Large margin; resistant to all expected dynamic load scenarios
1.50-1.99	Safe	Fit for operation; resistant to normal inertial loads
1.10-1.49	Marginal	Operate with caution; vulnerable to overload and dynamic loads
1.00-1.09	Critical	Near yielding; small inertial loads may exceed σ_y
< 1.00	Failure, yielding	Permanent plastic deformation; component must be withdrawn from service

RESULTS AND DISCUSSION

3.1. Scenario 1: Baseline Condition (0% Wear, 110% SWL)

The analytical nominal stress at the critical section was calculated using the Euler-Bernoulli beam model, with F = 37,770 N, L = 600 mm, b = 120 mm, and h = 60 mm. The analytical nominal bending stress was 314.8 MPa. The FEM simulation produced a maximum Von Mises stress of 487.1 MPa at the inner heel radius. The resulting Safety Factor was 1.745, which falls within the safe zone.

The FEM-based stress concentration factor was 1.548. This value was lower than the two-dimensional stepped-cantilever prediction by Pilkey and Pilkey (2008), which is typically in the range of 2.05-2.20. This difference is reasonable because the three-dimensional L-shaped fork geometry redistributes the stress field through triaxial constraint effects. The C3D10 solid element model captures multi-axial stress components, including transverse shear and Poisson effects, that are not represented in a simplified two-dimensional analytical model. The maximum tip deflection was 17.37 mm.

$$\sigma_{nom} = 6 F L / (b h^2) = 6(37{,}770)(600) / [120(60)^2] = 314.8 \text{ MPa}$$

$$K_t(FEM) = \sigma_{FEM} / \sigma_{nom} = 487.1 / 314.8 = 1.548$$

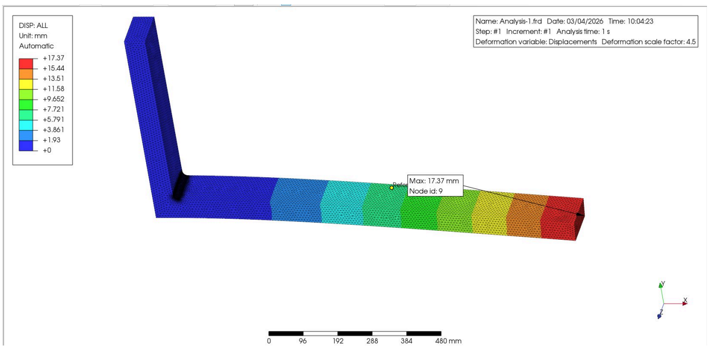

Image 1. Fork deflection contour for Scenario 1, 0% wear and 110% SWL. δmax = 17.37 mm, below the ISO 5057 limit of 36.36 mm.

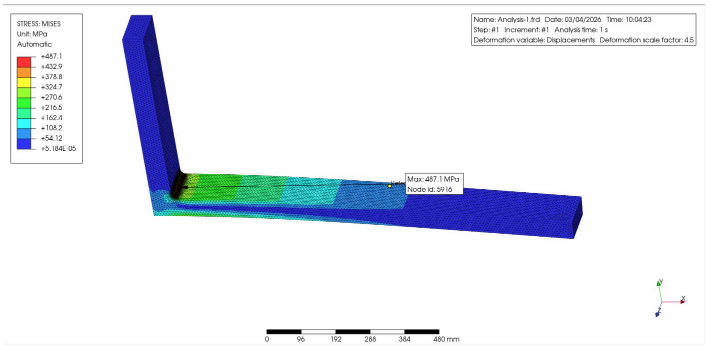

Image 2. Von Mises stress contour for Scenario 1. σVM = 487.1 MPa and SF = 1.745. Stress concentration occurs at the inner heel radius.

3.2. Scenario 2: Intermediate Wear (5% Wear, 100% SWL)

At 5% wear, the blade thickness decreased to 57.0 mm. The load was set to 100% SWL, equivalent to 34,335 N per fork. The FEM simulation produced a maximum Von Mises stress of 483.1 MPa and a Safety Factor of 1.759. This result also falls within the safe zone.

An important finding in this scenario is that the Von Mises stress was slightly lower than the baseline stress, even though the section was thinner. This occurs because the load decreased by 9.1% from the 110% SWL baseline to 100% SWL. This load reduction had a stronger effect than the stress increase caused by 5% thickness reduction. The result confirms that load level remains the dominant variable at low wear levels. The maximum tip deflection was 18.34 mm, which represents a 5.6% increase from the baseline.

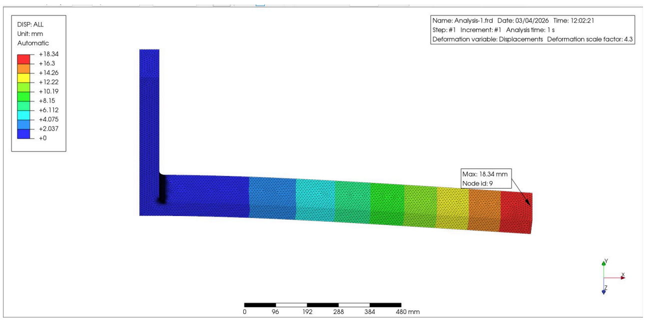

Image 3. Fork deflection contour for Scenario 2, 5% wear and 100% SWL. δmax = 18.34 mm, a 5.6% increase from the baseline.

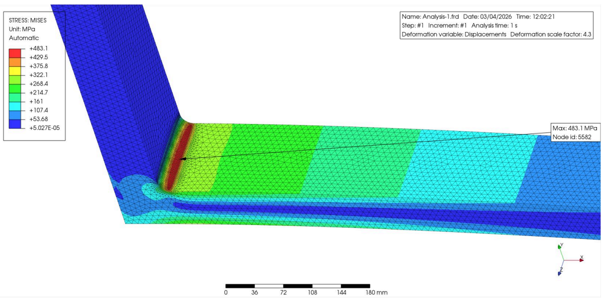

Image 4. Close-up of Von Mises stress in the inner heel radius for Scenario 2. σVM = 483.1 MPa and SF = 1.759.

3.3. Material Parameter Sensitivity Analysis

A material sensitivity analysis was performed because the inspection document did not specify the exact steel grade. The analysis used the critical 10% wear and 100% SWL condition, where the FEM stress was 528.9 MPa. The yield strength was varied from 655 MPa to 900 MPa, covering the reported range for AISI 4140 Q&T. The results are summarized in Table 6 and image 5. All tested yield strength values kept the fork within the elastic regime. However, the lower yield strength cases of 655 MPa and 750 MPa produced marginal Safety Factors. The conservative value of 850 MPa produced a Safety Factor of 1.607 and remained in the safe zone. This finding shows that the main conclusion is robust, but the safety classification depends strongly on the actual material strength.

Table 6. Safety Factor sensitivity to σy variation at 10% wear and 100% SWL

Case	σy (MPa)	SF at 10% wear, 100% SWL	Classification	Interpretation
S1	655	1.238	Marginal	Limited margin
S2	750	1.418	Marginal	Still limited margin
S3	850	1.607	Safe	Adequate margin
S4	900	1.702	Safe	Good margin

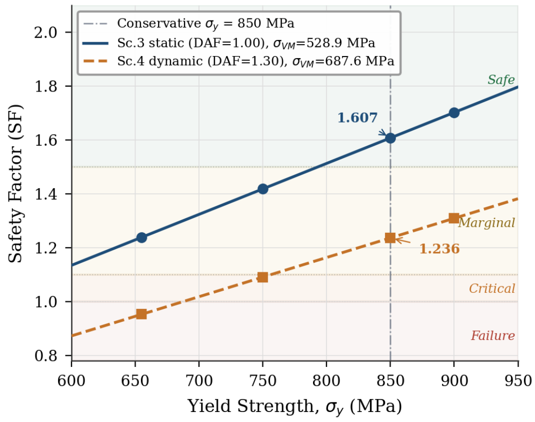

Image 5. Safety Factor sensitivity to AISI 4140 Q&T yield strength variation at 10% wear.

3.4. Scenario 3: Critical Wear (10% Wear, 100% SWL) and Regulatory Validation

At 10% wear, the blade thickness decreased to 54.0 mm. The FEM simulation produced a maximum Von Mises stress of 528.9 MPa and a static Safety Factor of 1.607. The fork remained in the safe elastic zone under static loading. The maximum tip deflection increased to 21.47 mm, or 23.6% higher than the baseline. A dynamic projection was then applied using DAF = 1.30. The effective stress increased to 687.6 MPa, and the Safety Factor decreased to 1.235. This value falls into the marginal zone. The safety margin erosion from Scenario 1 static condition to Scenario 3 dynamic projection was 29.2%. A further projection to 15% wear using the relationship $\sigma \propto 1/h^2$ produced an estimated Safety Factor of approximately 1.07 under dynamic loading, which approaches the critical zone. These results provide a mechanics-based explanation for the regulatory 10% wear limit. The limit should not be interpreted as an immediate failure boundary. Instead, it acts as an early-warning threshold. At 10% wear, the fork remains elastic under static loading, but its margin against dynamic effects has already decreased substantially. Therefore, withdrawal from service at the 10% wear threshold is rational and preventive.

σ_{eff} = DAF x σ_{FEM} = 1.30 x 528.9 = 687.6 MPa; SF = 850 / 687.6 = 1.235

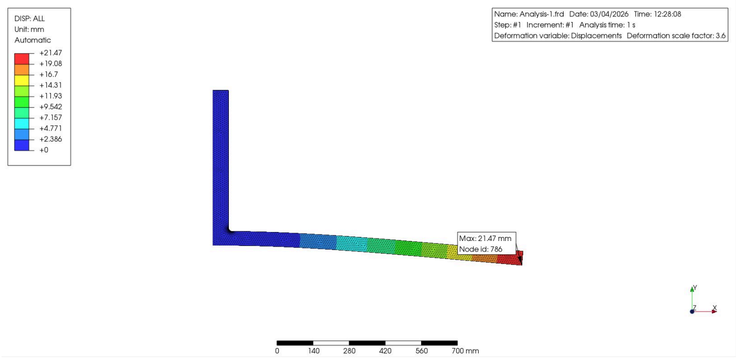

Image 6. Fork deflection contour for Scenario 3, 10% wear and 100% SWL. δmax = 21.47 mm, still below the ISO 5057 limit.

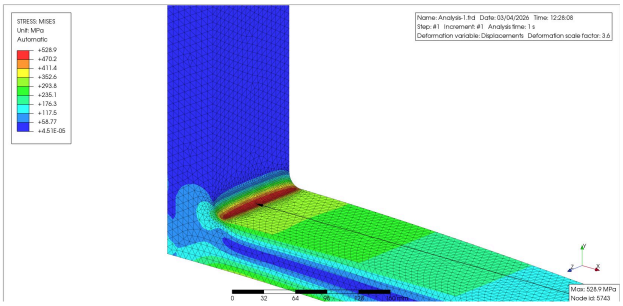

Image 7. Close-up of Von Mises stress in the inner heel radius for Scenario 3. σVM = 528.9 MPa and SF = 1.607.

3.5. Comparative Summary and Correlation with Field Data

The comparative summary of maximum Von Mises stress, Safety Factor, and structural status is presented in Table 7. All static scenarios remained in the safe elastic zone. The dynamic projection at 10% wear shifted the condition into the marginal zone, although the effective stress still did not exceed the conservative yield strength of 850 MPa. The correlation between field inspection data and FEM output is presented in Table 9. The MPI result of no indication is consistent with the simulated fully elastic condition. The satisfactory 110% SWL load test result also aligns with the Safety Factor of 1.745 in Scenario 1. Therefore, the FEM model does not replace field inspection. Instead, it strengthens the mechanical interpretation of field inspection results and provides a predictive view of safety margin degradation.

Table 7. Summary of peak Von Mises stress, Safety Factor, and structural status for all scenarios

Sc.	Wear	h (mm)	Load	DAF	σVM (MPa)	SF	Status
1	0%	60.0	110% SWL	1.00	487.1	1.745	Safe - elastic
2	5%	57.0	100% SWL	1.00	483.1	1.759	Safe - elastic
3	10%	54.0	100% SWL	1.00	528.9	1.607	Safe - elastic
4	10%	54.0	100% SWL	1.30	687.6	1.235	Marginal - elastic

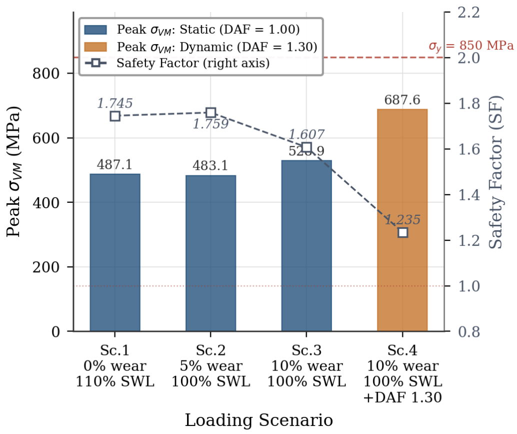

Image 8. Comparison of peak Von Mises stress and Safety Factor across all scenarios.

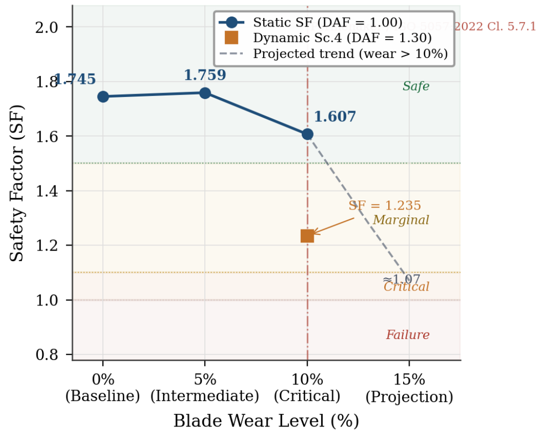

Image 9. Safety Factor degradation trend with blade wear level under static condition and dynamic projection.

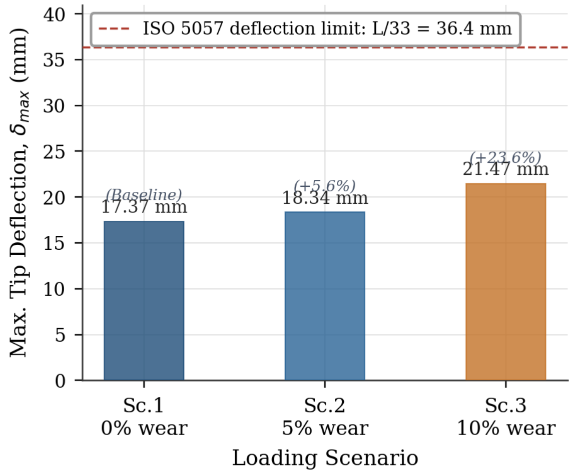

Image 10. Maximum deflection at the fork blade tip. All scenarios remain below the ISO 5057 deflection limit.

Table 8. Dynamic projection sensitivity analysis for Scenario 3, σFEM = 528.9 MPa

DAF	σeff (MPa)	SF = 850/σeff	Classification
1.15	608.2	1.397	Marginal
1.30	687.6	1.235	Marginal, reference case
1.40	740.5	1.148	Marginal, lower-bound margin

Note: all Safety Factor values in Table 8 fall within the marginal zone. This result strengthens the interpretation of the 10% wear limit as a mechanics-based early-warning threshold.

Table 9. Comparison matrix between empirical field data and computational FEM output

Parameter	Field result	FEM output	Status
NDT-MPI	No indication - pass (PT Dalaz, 2025b)	σVM < σy; fully elastic regime	Consistent; supports the absence of static crack indication
110% SWL load test	Satisfactory; no permanent deformation (PT Dalaz, 2025a)	SF = 1.745 at 110% SWL	Calibration consistency for σy = 850 MPa confirmed
10% wear limit	Mandatory withdrawal at wear >= 10% (Kementerian Ketenagakerjaan RI, 2020)	Static SF = 1.607; dynamic SF = 1.235	Early-warning threshold is mechanically justified

3.6. Research Limitations

This study has four main limitations. First, the linear static FEM model does not capture fatigue cycling that occurs during long-term operation. Second, the material was modeled as isotropic and homogeneous, so local variations caused by forging were not included. Third, eccentric loading, impact, and vibration during travelling were not modeled explicitly. The DAF value of 1.30 was used only as a conservative aggregate approximation. Fourth, the load distribution was assumed to be symmetric between the two fork arms, following static test conditions. Future studies should include fatigue analysis, transient dynamic simulation, eccentric loading, and experimental validation under actual operating conditions.

CONCLUSION

This study evaluated the structural safety margin degradation of Toyota 5FD70 forklift fork arms with a rated capacity of 7,000 kg using linear static FEM under three wear scenarios. Under the baseline condition of 0% wear and 110% SWL, the maximum Von Mises stress was 487.1 MPa and the Safety Factor was 1.745. This result is consistent with field data showing MPI no indication and a satisfactory load test. Under 5% wear and 100% SWL, the stress was 483.1 MPa and the Safety Factor was 1.759. The lower stress relative to baseline occurred because the load reduction had a stronger effect than the initial thickness reduction. At the critical 10% wear condition, the maximum Von Mises stress increased to 528.9 MPa and the static Safety Factor decreased to 1.607. The maximum deflection increased by 23.6% from the baseline, but it remained below the ISO 5057 deflection limit. A dynamic projection with DAF = 1.30 produced a Safety Factor of 1.235. This value indicates a 29.2% erosion of the safety margin from the baseline static condition and places the 10% wear condition in the marginal zone under dynamic projection. The findings support the 10% wear limit in Permenaker No. 08/2020 and ISO 5057:2022 as a mechanically justified early-warning threshold rather than a direct failure boundary. This conclusion applies within the scope of the Toyota 5FD70 unit, the assumed AISI 4140 Q&T material model, symmetric loading, and the linear static FEM formulation used in this study. For broader generalization, future research should include fatigue analysis, eccentric loading, and direct dynamic validation. FEM is recommended as a decision-support tool for inspection programs and risk-based forklift asset integrity management.

REFERENCES

ASM International. (1990). *ASM handbook: Volume 1, Properties and selection: Irons, steels, and high-performance alloys* (10th ed.). ASM International.

Bathe, K. J. (2014). *Finite element procedures* (2nd ed.). K. J. Bathe.

Borovinšek, M. (2025). *PrePoMax v2.4.0 manual*. University of Maribor.

Cascade Corporation. (2018). *Fork safety guide*. Cascade Corporation.

CEN. (2021). *EN 13001-2:2021 Crane safety: General design, Part 2: Load actions*. European Committee for Standardization.

Dhondt, G. (2024). *CalculiX CrunchiX user's manual version 2.22*. CalculiX.

Dowling, N. E. (2013). *Mechanical behavior of materials: Engineering methods for deformation, fracture, and fatigue* (4th ed.). Pearson.

Figueiredo, M. V., Oliveira, F. M. F., Gonçalves, J. P. M., de Castro, P. M. S. T., & Fernandes, A. A. (2001). Fracture analysis of forks of a heavy duty lift truck. *Engineering Failure Analysis, 8*(5), 411–421. https://doi.org/10.1016/S1350-6307(00)00040-6

ISO. (2002). *ISO 2330:2002 Fork-lift trucks: Fork arms: Technical characteristics and testing*. International Organization for Standardization.

ISO. (2022). *ISO 5057:2022 Industrial trucks: Inspection and repair of fork arms in service on fork-lift trucks*. International Organization for Standardization.

Massone, J. M., & Boeri, R. E. (2010). Failure of forklift forks. *Engineering Failure Analysis, 17*(5), 1062–1068. https://doi.org/10.1016/j.engfailanal.2009.12.005

Pantazopoulos, G., Vazdirvanidis, A., Rikos, A., & Toulfatzis, A. (2014). Analysis of abnormal fatigue failure of forklift forks. *Case Studies in Engineering Failure Analysis, 2*(1), 9–14. https://doi.org/10.1016/j.csefa.2013.12.005

Pilkey, W. D., & Pilkey, D. F. (2008). *Peterson's stress concentration factors* (3rd ed.). John Wiley & Sons.

Young, W. C., Budynas, R. G., & Sadegh, A. M. (2011). *Roark's formulas for stress and strain* (8th ed.). McGraw-Hill.

Zienkiewicz, O. C., Taylor, R. L., & Zhu, J. Z. (2013). *The finite element method: Its basis and fundamentals* (7th ed.). Butterworth-Heinemann.